



Article

Sinonasal Hyalinizing Adenoid Cystic Carcinoma Is Molecularly Different from Its Salivary and Breast Counterparts

Ebtissam Alerraqi ^{1,*}, Essam Mandour ² and Mariz Faltas ³

¹ Department of Pathology, Szeged University, H-6720 Szeged, Hungary

² Department of Pathology, Badr University in Cairo (BUC), Badr City 11829, Egypt

³ Department of Oral Pathology, Misr University for Science and Technology, Giza 3236101, Egypt

* Correspondence: ebtissam.erraqi@gmail.com

Abstract: Adenoid cystic carcinoma (AdCC) is known to behave differently based on its location, histologic features, and molecular profile. Despite this understanding, efforts to use these molecular findings to develop personalized treatments have not yet been successful. The purpose of this retrospective study is to examine the molecular characteristics of AdCC with various histologic features in three different locations. A reference group of 20 classic cribriform AdCC cases from the parotid gland was included, along with 10 salivary AdCCs (Group 1), 10 sinonasal AdCCs with hyalinization (Group 2), and 10 solid mammary AdCCs with basaloid features (Group 3). Tissue samples were processed and tested using various molecular techniques, and the Wilcoxon signed-rank test was used to compare the different groups. Molecular data were obtained for both common and rare cases of sinonasal, salivary, and mammary AdCCs, revealing differences in molecular features depending on the tumor's location. The molecular profile of the AdCCs in the experimental group varied depending on the site, with MYB gene rearrangements being common in all cases. We report the first MYB::KMT2C/D fusions in a subset of salivary AdCCs and sinonasal AdCCs but not in mammary adenoid cystic carcinoma with basaloid features. We conclude that co-occurring genetic alterations may vary among different sites and may have implications for the prognosis and treatment plan of AdCC. More research is needed to fully understand the mechanisms of KMT2C and KMT2D mutations in the development and progression of head and neck cancer, including their interactions with the NOTCH pathway.

Keywords: adenoid cystic carcinoma; salivary; sinonasal; hyalinization; solid mammary; basaloid features



Citation: Alerraqi, E.; Mandour, E.; Faltas, M. Sinonasal Hyalinizing Adenoid Cystic Carcinoma Is Molecularly Different from Its Salivary and Breast Counterparts. *J. Mol. Pathol.* **2023**, *4*, 89–98. <https://doi.org/10.3390/jmp4020010>

Academic Editor: Giancarlo Troncone

Received: 30 January 2023

Revised: 28 April 2023

Accepted: 8 May 2023

Published: 15 May 2023



Copyright: © 2023 by the authors. Licensee MDPI, Basel, Switzerland. This article is an open access article distributed under the terms and conditions of the Creative Commons Attribution (CC BY) license (<https://creativecommons.org/licenses/by/4.0/>).

1. Introduction

Adenoid cystic carcinoma (AdCC) demonstrates diverse morphology and molecular profiling. Conventional AdCC is a rare, biologically unique biphasic tumor that consists of malignant myoepithelial and luminal cells. High-grade transformations reveal greater nuclear enlargement and irregularity and higher mitotic counts than conventional AdCC. High-grade AdCC does not reveal biphasic ductal–myoepithelial differentiation [1]. Solid and basaloid adenoid cystic carcinoma (SB-AdCC) is considered a rare aggressive variant of mammary AdCC, with a higher incidence of distant metastases than salivary AdCC [2]. In SB-AdCCs lacking MYB rearrangements, CREBBP, KMT2C, and NOTCH1 alterations were observed in 50% of cases [3]. Less than 25% of the SB-AdCCs displayed the genomic features of salivary AdCC.

Sinonasal AdCC illustrates histologic features that diverge from their counterparts in other topographies. Metatypical AdCC with keratinization [4] and sebaceous differentiation [5] were considered characteristic of the nasal cavity. AdCC collided with many histologically distinct and topographically independent carcinomas, including head and neck squamous cell carcinoma [6], while sinonasal AdCC collided with premalignant lesions,

including sinonasal inverted papilloma [7]. In addition, hybrid AdCC in the nasopharynx is more frequent than in the oral cavity [8]. Epithelial–myoepithelial carcinomas (EMCs) and AdCC are often associated, posing questions about the tumor–tumor interaction and the accuracy of the diagnosis of each tumor [9]. Even human papillomavirus-related multiphenotypic sinonasal carcinoma (HMSC) [10–13], which was expected to arise in the nasal cavity, was recently reported in the breast [14].

Similar to the detection of the *CRTC1/3::MAML2* fusion gene in both mucoepidermoid carcinoma (MEC) and cutaneous MEC [15], other than hidradenoma [16], the *MYB::NFIB* gene fusion is a novel genetic link between adenoid cystic carcinoma and dermal cylindroma [17]. Comparing adenoid cystic carcinoma from the salivary gland and breast identified 31 upregulated and 62 downregulated miRNAs, of which none was native-tissue-specific [18].

Therefore, the changing behavior of AdCC according to site, histologic features, and molecular profile is now evident. The possibility of translating molecular findings into therapeutic implications during the era of personalized medicine has so far been unsuccessful. Moreover, defining whether these tumors represent a subtype of AdCC or a collection of cancer types with a similar basaloid histologic appearance is warranted. We aim to investigate the molecular analysis of AdCC, which depicts various histologic features in three topographies. Developing drugs that can selectively target *MYB* without affecting normal cellular processes has been a significant challenge. Targeting *MYB* may require a combination of approaches, including drugs that target its upstream regulators or downstream targets, in addition to direct *MYB* inhibitors. In this study, we aim to define new genetic fusion partners.

2. Materials and Methods

Despite advances in treatment strategies, including surgery, radiotherapy, and chemotherapy, AdCC remains an incurable cancer. This is because the cancer cells have a unique ability to invade and grow around nerves and blood vessels, making complete surgical removal nearly impossible. By understanding the specific molecular drivers of AdCC in each location, targeted therapies can be developed to specifically address those drivers. For example, clinical trials are currently ongoing to evaluate the efficacy of *MYB* inhibitors for treating AdCCs with *MYB* alterations. Similarly, the use of specific molecular markers can aid in the diagnosis and prognosis of AdCC, allowing for more tailored and individualized treatment plans. In this retrospective study, we collected a reference group of 20 cases of classic cribriform AdCCs of the parotis, 10 salivary AdCCs with unusual features (Group 1), 10 sinonasal AdCCs with hyalinization (Group 2), and 10 solid mammary AdCCs with basaloid features. The unusual morphological characteristics of AdCC can include hyaline globules, which are small, round, eosinophilic structures that can be found within the tumor cells or stroma. Additionally, AdCC can sometimes contain areas of necrosis or cystic change, which can further complicate diagnosis and treatment. When this is the case, the stroma of ACC can appear hyalinized, which means that it is thickened and glassy in appearance. AdCC can have areas of high cellularity, with densely packed tumor cells, as well as areas of low cellularity, with scattered tumor cells.

The paraffin wax blocks were sectioned to be stained with SOX10 (BC34, Mouse, 1:200, Cell Marque), CK7: (OV-TL 12/30, Mouse, 1:200, Dako), CD117: (YR145, Rabbit, 1:200, Abcam), and p63 (4A4, Mouse, 1:200, Cell Marque). All formalin-fixed, paraffin-embedded tissue samples were molecularly tested using FISH SPEC *MYB* Dual Color Break Apart Probe (ZytoLight®, ZytoVision GmbH, Bremerhaven, Germany), which detects the *MYB* translocation harboring on 6q23.3 and next-generation sequencing.

NGS is a high-throughput technology that allows simultaneous detection of various genetic alterations in a sample. To detect *MYB* gene fusion, the tissue samples for sequencing were prepared for extracting and purifying the RNA from the samples and preparing them for library preparation. We then used a commercial kit that fits the adapter ligation, fragmentation, and PCR amplification. RNA-Seq was performed using Illumina's

TruSight RNA Fusion Panel and a MiSeq or NextSeq sequencer (at least 2 million reads per sample) according to the manufacturer's recommendations (Illumina, San Diego, CA, USA). We selected all fusion RNAs as candidates for pathogenic fusion transcripts. After sequencing, the data were analyzed to identify MYB gene fusions with a reference based on the presence of chimeric reads that span the fusion junction. The gene list is available at www.illumina.com (accessed on 13 March 2023).

For verification of NGS, we used FISH SPEC *KMT2C* and *KMT2D* Color break apart probes (Empire Genomics[®], USA) to detect any translocations. The probes are designed using fluorescently labeled DNA oligonucleotides that are complementary to the target regions of *KMT2C* and *KMT2D* genes. The probes are labeled with different fluorophores to create a color break-apart signal. The probes were mixed with denatured target DNA on a slide and allowed to hybridize. The excess probe was washed away, and the slide was counterstained with a DNA stain to visualize the chromosomes. Two hundred successive nuclei were examined. Detection of a sufficient break-apart signal was interpreted as a positive score. The Wilcoxon signed-rank test was used to compare the studied groups.

3. Results

In this study, a reference group consisting of 10 conventional low-grade parotid AdCCs seen in adults, with a peak incidence in the 5th and 6th decades of life, was used for comparison (not shown in Table 1). This reference group showed no perineural invasion and displayed a sieve-like growth pattern, where the tumor cells formed small, round, glandular spaces separated by thin, delicate fibrous septae. The spaces were typically filled with mucin and basophilic material, and the tumor cells appeared small and uniform with round to oval nuclei and scant cytoplasm. The nuclei were hyperchromatic with inconspicuous nucleoli, and focal nuclear pleomorphism and mitotic figures were inconspicuous. While it is typical for AdCC to manifest in minor salivary glands and invade the nerves, we chose to focus on AdCC of a single major gland (the parotid gland) with no discernible morphologies. This approach allows us to determine whether these histologic features are significant predisposing factors for site-specific molecular alterations. Molecularly, AdCC is characterized by a t(6;9)(q22-23;p23-24) chromosomal translocation that results in the fusion of the MYB proto-oncogene with the *NFIB* gene. The purpose of using this reference group was to establish a baseline for comparison with the experimental group, which may have had different or unique features that needed to be identified and analyzed. The reference group served as a reference point to determine if any observed differences in the experimental group were significant or not.

For the experimental group, the majority of the sample was male (16/30) and the age of both genders ranged from 34 to 72 years. The AdCC was located in several different sites including the sinonasal area, the minor salivary gland, the parotid gland, the submandibular gland, and the breast. The members of the subgroups were distributed equally among those with AdCC in the breast (10/30), the sinonasal area (10/30), and the salivary gland (10/30), of which minor and major salivary gland incidence was proportioned. Female patients with sinonasal AdCC in the area demonstrated rearrangements of the MYB gene detected by FISH, with most of them having *MYB::NFIB* or *MYB::KMT2D* fusion genes. This is a common finding in AdCC of the sinonasal area and was associated with a favorable prognosis. In contrast, the patients with AdCC in the minor salivary glands, parotid gland, and breast have a more varied molecular profile. Most of these patients have rearrangements of the MYB gene detected by FISH, but some have a retained MYB gene. In addition, some of these patients have rearrangements of the *KMT2D* or *KMT2C* genes detected by FISH.

Table 1. Clinicopathological profile of the studied cases.

Case	Sex/Age	Diagnosis/Site	Histologic Features	MYB/FISH	NGS	KMT2D/FISH	KMT2C/FISH
1	F/44	AdCC/sinonasal	Hyalin, CC	Rearranged	MYB::NFIB, MYB::KMT2D	Rearranged	Retained
2	M/44	AdCC/sinonasal	Hyalin, CC	Rearranged	MYB::NFIB	Rearranged	Retained
3	F/39	AdCC/sinonasal	Hyalin, CC	Rearranged	MYB::NFIB, MYB::KMT2D	Rearranged	Retained
4	F/40	AdCC/sinonasal	Hyalin, scler.	Rearranged	MYB::NFIB, MYB::KMT2D	Not analyzable	Retained
5	F/54	AdCC/sinonasal	Hyalin, CC	Rearranged	MYB::NFIB, MYB::KMT2D	Rearranged	Retained
6	M/42	AdCC/sinonasal	Hyalin, CC	Rearranged	Not analyzable	Rearranged	Retained
7	F/64	AdCC/sinonasal	Hyalin, scler.	Rearranged	MYB::NFIB, MYB::KMT2D	Rearranged	Retained
8	F/59	AdCC/sinonasal	Hyalin, CC	Rearranged	MYB::NFIB, MYB::KMT2D	Rearranged	Retained
9	M/43	AdCC/sinonasal	Hyalin, CC	Rearranged	MYB::NFIB	Rearranged	Retained
10	F/52	AdCC/sinonasal	Cribri, trabec	Rearranged	MYB::NFIB	Not analyzable	Retained
11	M/40	AdCC/minor SG	Cribri, scler	Rearranged	MYB::NFIB, MYB::KMT2C	Retained	Rearranged
12	F/51	AdCC/minor SG	Cribri	Rearranged	MYB::NFIB, MYB::KMT2C	Retained	Rearranged
13	M/42	AdCC/minor SG	Cribri	Rearranged	Not analyzable	Retained	Rearranged
14	M/43	AdCC/minor SG	Cribri, CC	Rearranged	Not analyzable	Retained	Not analyzable
15	M/72	AdCC/minor SG	Cribri, solid	Rearranged	MYB::NFIB, MYB::KMT2C	Retained	Rearranged
16	M/34	AdCC/parotis	Cribri	Rearranged	MYB::NFIB, MYB::KMT2C	Retained	Rearranged
17	M/48	AdCC/ parotis	Cribri	Rearranged	MYB::NFIB, MYB::KMT2C	Retained	Rearranged
18	F/40	AdCC/ parotis	Cribri, trabec	Rearranged	MYB::NFIB	Retained	Not analyzable
19	M/60	AdCC/ parotis	Cribri	Rearranged	MYB::NFIB	Retained	Not analyzable
20	M/49	AdCC/SBG	Solid, basaloid	Rearranged	MYB::NFIB	Retained	Retained
21	M/42	AdCC/breast	Solid, basaloid	Rearranged	MYB::NFIB	Retained	Retained
22	F/57	AdCC/breast	Solid, basaloid	Retained	Not analyzable	Retained	Retained
23	M/42	AdCC/breast	Solid, basaloid	Rearranged	MYB::NFIB	Retained	Retained
24	M/42	AdCC/breast	Solid, basaloid	Rearranged	MYB::NFIB	Retained	Retained
25	F/42	AdCC/breast	Solid, basaloid	Rearranged	MYB::NFIB	Retained	Retained
26	F/47	AdCC/breast	Solid, basaloid	Rearranged	MYB::NFIB	Retained	Retained
27	M/44	AdCC/breast	Solid, basaloid	Rearranged	MYB::NFIB	Retained	Retained
28	M/63	AdCC/breast	Solid, basaloid	Retained	Not analyzable	Retained	Retained
29	F/72	AdCC/breast	Solid, basaloid	Retained	Not analyzable	Retained	Retained
30	F/43	AdCC/breast	Solid, basaloid	Rearranged	Not analyzable	Retained	Retained

Abbreviations: AdCC: Adenoid cystic carcinoma; CC: clear cells; Cribri: Cribriiform; Hyalin: hyalinization; SBG: submandibular gland; scler: sclerosis. Studied cases were viewed with caution.

Histologically, salivary nonsolid AdCCs showed biphasic cell populations arranged in alternate cribriform and tubular architectures (Figure 1). The cribriform pattern demonstrated nests of neoplastic cells with hyperchromatic, angulated nuclei arranged in microcystic and macrocystic spaces. These pseudocystic cavities were occasionally filled with hyaline or basophilic mucoid material. The histologic features in the major salivary glands did not differ much from those in the minor salivary glands. However, solid nests of AdCC favored submucosal infiltration in the minor salivary glands (Figure 2, Case #15).

Sinonasal AdCC revealed nests of cribriform and solid areas, while extensive hyalinization was recapitulating a jigsaw puzzle-like pattern (Figure 3). The cells of sinonasal AdCC were sometimes basaloid, with dark, hyperchromatic nuclei. The cells were typically arranged in a palisading pattern around the cystic spaces. A few salivary AdCCs revealed basaloid cells arranged in solid growth patterns that were insufficient for diagnosis as high-grade AdCCs. Mammary SB-AdCC revealed areas of cribriform, a solid growth pattern (>90%), and a basaloid appearance, with myxoid or hyalinized stroma. Ductules were present within the tumor islands. Small cysts and pseudoglandular structures were occasionally seen (Figure 4). This variant is characterized by the presence of small, basal-like cells with scant cytoplasm. The basaloid variant was associated with a higher risk of metastasis and a poorer prognosis. All neoplastic cells were positive for IHC SOX10, CK7, CD117, p63, and KI67. The clinical and molecular findings are shown in Table 1. There, all of the AdCC cases had MYB rearrangements detected by fluorescence in situ hybridization (FISH), which is a common genetic alteration observed in AdCC. Specifically, MYB was found to be fused with *NFIB* and/or *KMT2C/KMT2D* in AdCC cases from sinonasal and minor SG sites. *MYB::NFIB* fusion is a well-known molecular alteration that occurs in approximately 30–70% of AdCC cases and has been associated with better prognosis compared to cases without this fusion. On the other hand, *MYB::KMT2C/D* fusions were less common but have also been reported in cases from salivary and sinonasal AdCCs. Although this is the first study to report this finding, its clinical significance is yet to be fully elucidated. In addition to FISH, some AdCC cases were also analyzed using next-generation sequencing. In Table 1, NGS was performed in several AdCC cases from sinonasal, minor SG, and parotid gland sites. *MYB::NFIB* and *MYB::KMT2D* fusions were detected in these cases, which is consistent with the FISH results. Notably, some cases were not analyzable by NGS, which may be due to various reasons such as low DNA quality or quantity. The median score for Group 1 was 70 (IQR: 60–80), the median score for Group 2 was 85 (IQR: 75–90), and the median score for Group 3 was 60 (IQR: 55–70). The results indicate that there was a significant difference between Group 1 and Group 3 ($p < 0.05$) and between Group 2 and Group 3 ($p < 0.05$) but not between Group 1 and Group 2 ($p > 0.05$). This suggests that the solid mammary AdCCs with basaloid features (Group 3) have different characteristics compared to the other two groups.

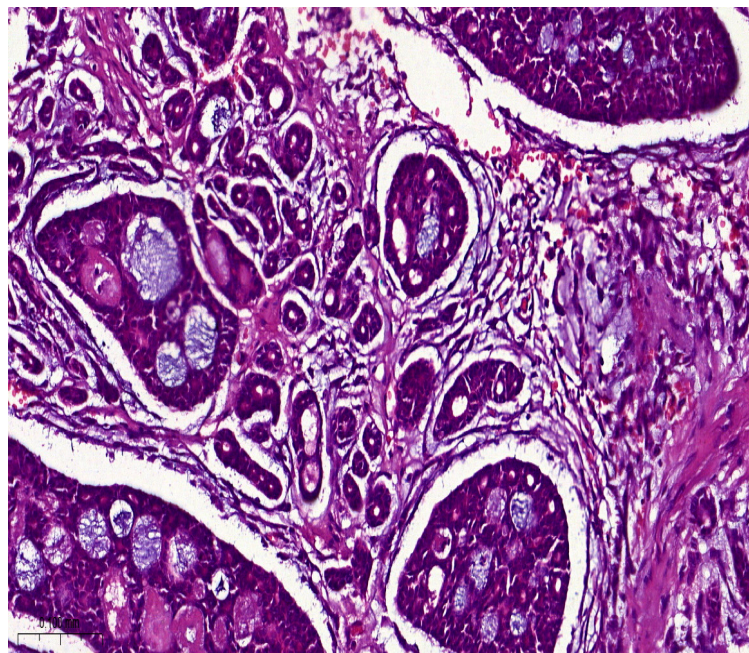


Figure 1. Salivary AdCC showed biphasic cell populations arranged in alternate cribriform and tubular architectures. Pseudocystic cavities were occasionally filled with hyaline or basophilic mucoid material (H&E stain; magnification $\times 5$).

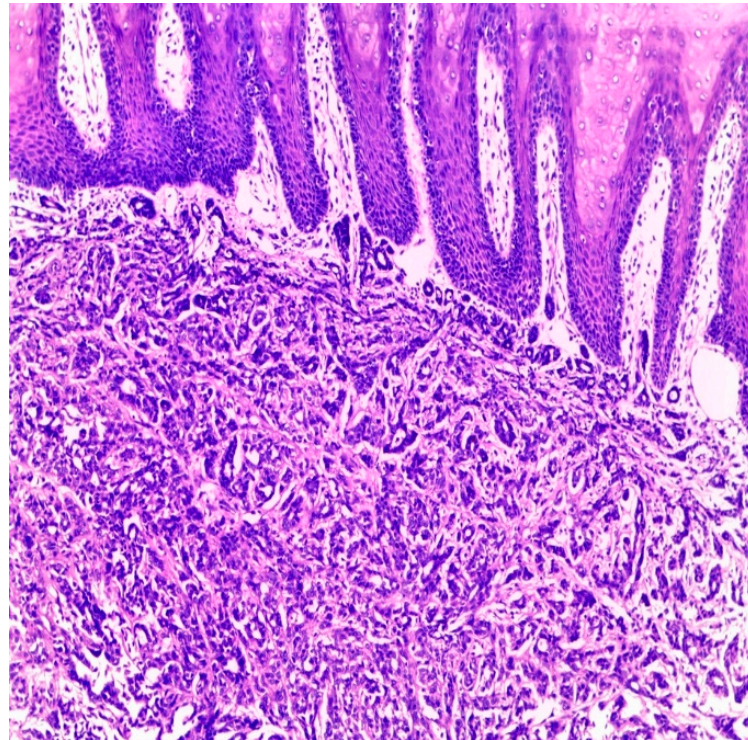


Figure 2. AdCC of minor salivary gland with submucosal infiltration by solid nests (H&E stain; magnification $\times 5$).

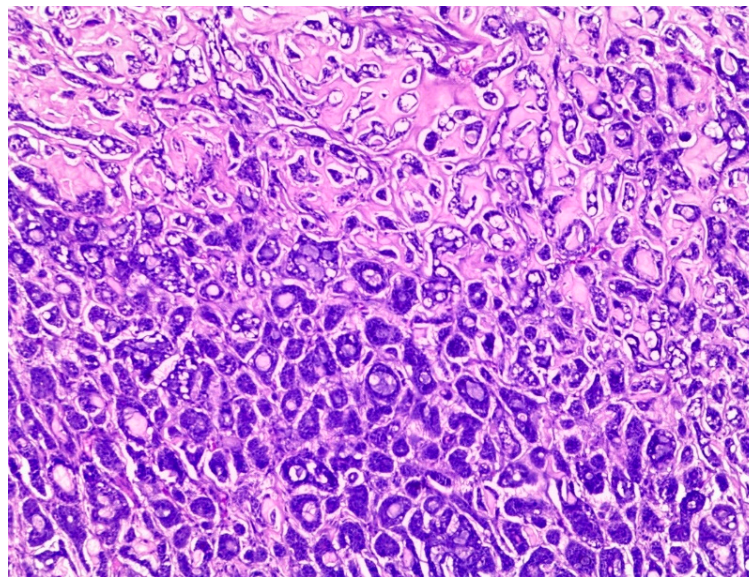


Figure 3. Sinonasal AdCC revealed nests of cribriform and solid areas, while extensive hyalinization was recapitulating a jigsaw puzzle-like pattern (H&E stain; magnification $\times 5$).

As researchers continue to investigate and develop new techniques, they may uncover additional molecular alterations that were previously unknown. There is no end in sight for the discovery of new molecular alterations, and this process may continue in the foreseeable future. However, relating molecular findings to changing clinical behaviors is mandatory.

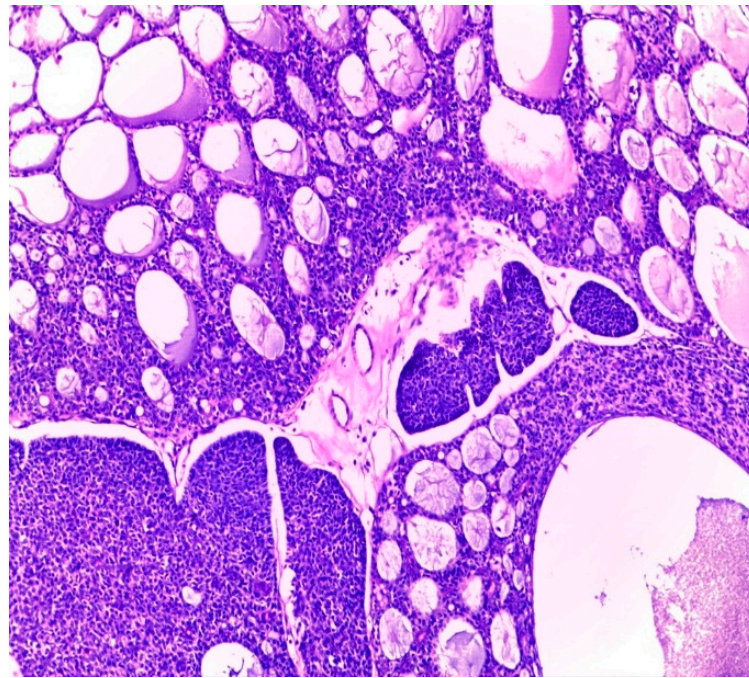


Figure 4. Mammary SB-AdCC revealed areas of cribriform, a solid growth pattern (>90%), and a basaloid appearance, with myxoid or hyalinized stroma. Ductules were present within the tumor islands (H&E stain; magnification $\times 5$).

4. Discussion

AdCCs share common ground regardless of the affected site. However, some topographies have shown particular molecular and histologic features that could be associated with more or less favorable prognosis. The successful identifications of these differences could prove effective in customizing therapeutic modalities.

Our results have identified that both the presence of MYB translocation and the level of MYB protein expression are associated with higher recurrence rates and a worse prognosis. Studies have shown that almost all AdCC patients have oncogenic fusion and the overexpression of the Myb or Mybl1 gene [19]. MYB translocation is not specific to AdCC, and it is sensitive to diffuse low-grade pediatric glioma and leukemia, the blockage of which has produced promising therapeutic outcomes in vitro. Examples of therapeutic drugs include conensin, salinomycin, and nigericin [20], which inhibit the NOTCH1-HEY1 pathway [21].

Personalized medicine has been increasingly successful in translating molecular findings into therapeutic implications. Several targeted therapies, such as tyrosine kinase inhibitors and monoclonal antibodies, have been developed based on specific genetic alterations found in cancer patients. For instance, the use of trastuzumab, a monoclonal antibody targeting the HER2 protein, has significantly improved the outcomes of breast cancer patients with HER2-positive tumors. Furthermore, the advancement of precision medicine has enabled the identification of specific subgroups of patients that are more likely to benefit from certain therapies. For example, patients with lung cancer whose tumors have specific mutations in the EGFR gene are more likely to respond to EGFR inhibitors, such as gefitinib and erlotinib. Although there are still challenges and limitations to personalized medicine, such as the need for better biomarkers and the high cost of targeted therapies, targeting MYB is challenging because it is an intracellular protein that regulates gene expression by binding to DNA, making it difficult to design small molecule drugs that can specifically target MYB. Therefore, identifying as many fusion partners as possible is therapeutically impactful.

KMT2 family proteins (*SET1A*, *SET1B*, *MLL1/KMT2A*, *MLL4/KMT2B*, *MLL3/KMT2C*, and *MLL2/KMT2D*) provide the histone lysine methyltransferase activity of mammalian

COMPASS complexes. The *KMT2C* and *KMT2D* COMPASS-like (MLR) complexes monomethylate H3K4 (H3K4me1) at transcription enhancers throughout the human genome. The brain-specific knockout of *Kmt2d* in mice is associated with spontaneous medulloblastoma, perhaps via the hyperactivation of the Ras and Notch pathways and the downregulation of tumor suppressor genes. The dysregulation of *KMT2C* and *KMT2D* has been linked to several types of cancer, including leukemia, lymphoma, and solid tumors. *KMT2C/D* mutations can lead to the aberrant activation of the NOTCH pathway. For example, *KMT2D* mutations have been found to increase the expression of NOTCH target genes in B-cell lymphoma.

AdCC with mutations in Notch-1, an overexpression of MYC, and an upregulation of the mRNA splicing pathway are devoid of myoepithelial cells and behave aggressively [22]. Either salivary [23–25], sinonasal, or breast AdCCs show MYB pathway activation, usually underpinned by the *MYB::NFIB* fusion gene [26]. However, the variable histologic features pertaining to the corresponding clinical aggressiveness are the main focus of recent studies for identifying the oncogenic pathways with blockages that could ameliorate the destructive behavior of the tumor and improve its prognosis [27]. The lack of MYB translocation in mammary adenoid cystic carcinoma with basaloid features may be due to different pathogenic mechanisms, such as alterations in NOTCH signaling or other genetic pathways. However, we did not demonstrate *KMT2C/D* in our analyzed cases.

High-grade transformations show characteristics that are consistent with myoepithelial differentiation and a high rate of proliferation in the presence of SMA, p63, and calponin and are high on the Ki-67 index, which is usually associated with aggressive, malignant, or high-grade tumors [28]. Notch pathway activation is the most frequent alteration, in addition to *MYB* or *MYBL1*, with shorter disease-free and worse outcomes in Notch wild-type mutated AdCC. One study's results suggest that the Ki-67 index and high AgNOR were concurrent with poor prognoses [29]. Additionally, *BCOR* and *KMT2C* mutations in *RUNX1* were considered to be of good prognostic value for the cribriform variant.

One of the major challenges in managing AdCC is the lack of good predictive markers that can help identify which patients are at a higher risk of recurrence or metastasis. Currently, there are no reliable biomarkers or genetic markers that can predict the behavior of AdCC or its response to treatment. This makes it difficult for physicians to tailor treatment plans and surveillance strategies for individual patients, and it also makes it challenging to develop new treatments for AdCC. Immunohistochemically, there are several AdCC markers that have valuable prognostic values. For example, the *Sema3A* gene, a secreted protein with odontogenic and oncogenic functions, is strongly expressed in the cytoplasm of AdCC tumor cells and could be a specific marker for myoepithelial neoplastic cells in AdCC. The elevated expression of *Sema3A* might activate AKT signaling and enhance cell proliferation in AdCC [30]. Yet, relating the clinicopathological findings to molecular labeling is mandatory in salivary gland carcinomas [31].

5. Conclusions

We retrieved genetic data corresponding to 30 cases of AdCC. The genetic profiles of the studied cases of sinonasal, salivary, and mammary AdCC showed different molecular findings. However, specific MYB fusion partners and other co-occurring genetic alterations may vary among different sites and may have implications in the prognosis and treatment plan of AdCC. Therefore, the comprehensive molecular profiling of AdCC is crucial for better understanding the biology of this rare malignancy and for developing personalized treatment strategies. According to our findings, *MYB::KMT2D* is a novel alteration in sinonasal AdCC, while *MYB::KMT2D* is a novel alteration in salivary AdCC. This could be useful in customizing target-specific therapeutic modalities. We hold the conviction that examining three groups of AdCC of diverse sites and morphologies is crucial for acquiring a profound comprehension of the potentially novel target genes implicated in the oncogenesis of AdCC phenotypes. Accordingly, we urge authors to undertake a multi-institutional analysis to further scrutinize this discovery.

Questions regarding the diverse molecular profile of AdCCs according to the site seem to be warranted. Furthermore, it is unclear if the co-targeting pathways involved in, in particular, topographies should be framed withing taxonomical subtyping or topographical specificity. Further evidence is still needed to characterize *KMT2C*- and *KMT2D*-arranged AdCC. Further research is needed to fully understand the mechanisms by which *KMT2C* and *KMT2D* mutations contribute to the development and progression of head and neck cancer, including their interactions with the NOTCH pathway.

Author Contributions: Conceptualization, E.A.; methodology, E.A.; validation, E.A., E.M. and M.F.; formal analysis, E.A. and M.F.; investigation, E.A. and M.F.; resources, E.A. and M.F.; data curation, E.A. and E.M.; writing—original draft preparation, E.A. and M.F.; writing—review and editing, E.A., E.M. and M.F.; visualization, E.A. and E.M.; supervision, E.A. and E.M.; project administration, E.A. All authors have read and agreed to the published version of the manuscript.

Funding: This research received no external funding.

Institutional Review Board Statement: Obtained from Badr University in Cairo (BUC), Egypt.

Informed Consent Statement: Not applicable.

Data Availability Statement: The data presented in this study are available on request from the corresponding author.

Conflicts of Interest: The authors declare no conflict of interest.

References

- Seethala, R.R.; Hunt, J.L.; Baloch, Z.W.; LiVolsi, V.A.; Leon Barnes, E. Adenoid cystic carcinoma with high-grade transformation: A report of 11 cases and a review of the literature. *Am. J. Surg. Pathol.* **2007**, *31*, 1683–1694. [[CrossRef](#)] [[PubMed](#)]
- D'Alfonso, T.M.; Mosquera, J.M.; Macdonald, T.Y.; Padilla, J.; Liu, Y.F.; Rubin, M.A.; Shin, S.J. MYB-NFIB gene fusion in adenoid cystic carcinoma of the breast with special focus paid to the solid variant with basaloid features. *Hum. Pathol.* **2014**, *45*, 2270–2280. [[CrossRef](#)] [[PubMed](#)]
- Schwartz, C.J.; Brogi, E.; Marra, A.; Da Cruz Paula, A.F.; Nanjangud, G.J.; da Silva, E.M.; Patil, S.; Shah, S.; Ventura, K.; Razavi, P.; et al. The clinical behavior and genomic features of the so-called adenoid cystic carcinomas of the solid variant with basaloid features. *Mod. Pathol.* **2022**, *35*, 193–201. [[CrossRef](#)] [[PubMed](#)]
- Mathew, E.P.; Todorovic, E.; Truong, T.; Dickson, B.C.; Enepekides, D.; Poon, I.; Weinreb, I. Metatypical Adenoid Cystic Carcinoma A Variant Showing Prominent Squamous Differentiation with a Predilection for the Sinonasal Tract and Skull Base. *Am. J. Surg. Pathol.* **2021**, *46*, 816–822. [[CrossRef](#)]
- Ooms, K.; Chiosea, S.; Lamarre, E.; Shah, A. Sebaceous Differentiation as Another Feature of Metatypical Adenoid Cystic Carcinoma: A Case Report and Letter to the Editor. *Am. J. Surg. Pathol.* **2023**, *47*, 145–146. [[CrossRef](#)]
- Ogane, S.; Kawano, T.; Hiraga, C.; Suzuki, T.; Hashimoto, K.; Nomura, T. Oral collision cancer: A case report and literature review of simultaneous squamous cell and adenoid cystic carcinoma of the oral mucosa. *Oral Sci. Int.* **2022**, *19*, 123–128. [[CrossRef](#)]
- Takada, Y.; Asako, M.; Kawachi, R.; Takada, T.; Iwai, H. Sinonasal Inverted Papilloma Associated with Adenoid Cystic Carcinoma. *Case Rep. Oncol.* **2021**, *14*, 1429–1434. [[CrossRef](#)]
- Woo, J.S.; Kwon, S.Y.; Jung, K.Y.; Kim, I. A hybrid carcinoma of epithelial-myoepithelial carcinoma and adenoid cystic carcinoma in maxillary sinus. *J. Korean Med. Sci.* **2004**, *19*, 462–465. [[CrossRef](#)]
- Bishop, J.A.; Westra, W.H. MYB Translocation Status in Salivary Gland Epithelial-Myoepithelial Carcinoma. *Am. J. Surg. Pathol.* **2018**, *42*, 319–325. [[CrossRef](#)]
- Bishop, J.A.; Westra, W.H. Human papillomavirus-related multiphenotypic sinonasal carcinoma: An emerging tumor type with a unique microscopic appearance and a paradoxical clinical behaviour. *Oral Oncol.* **2018**, *87*, 17–20. [[CrossRef](#)]
- Rooper, L.M.; McCuiston, A.M.; Westra, W.H.; Bishop, J.A. SOX10 Immunoexpression in Basaloid Squamous Cell Carcinomas: A Diagnostic Pitfall for Ruling out Salivary Differentiation. *Head Neck Pathol.* **2019**, *13*, 543–547. [[CrossRef](#)] [[PubMed](#)]
- Shah, A.A.; Lamarre, E.D.; Bishop, J.A. Human Papillomavirus-Related Multiphenotypic Sinonasal Carcinoma: A Case Report Documenting the Potential for Very Late Tumor Recurrence. *Head Neck Pathol.* **2018**, *12*, 623–628. [[CrossRef](#)] [[PubMed](#)]
- Shah, A.A.; Oliyai, B.R.; Bishop, J.A. Consistent LEF-1 and MYB Immunohistochemical Expression in Human Papillomavirus-Related Multiphenotypic Sinonasal Carcinoma: A Potential Diagnostic Pitfall. *Head Neck Pathol.* **2019**, *13*, 220–224. [[CrossRef](#)] [[PubMed](#)]
- Oramas, D.M.; Bell, D.; Middleton, L.P. Sinonasal analogue HPV related breast multiphenotypic carcinoma, a report of a case with the first description in the breast. *Diagn. Pathol.* **2020**, *15*, 1–5. [[CrossRef](#)] [[PubMed](#)]
- Lennerz, J.K.M.; Perry, A.; Dehner, L.P.; Pfeifer, J.D.; Lind, A.C. CRTCl rearrangements in the absence of t(11;19) in primary cutaneous mucoepidermoid carcinoma. *Br. J. Dermatol.* **2009**, *161*, 925–929. [[CrossRef](#)]

16. Kuma, Y.; Yamada, Y.; Yamamoto, H.; Kohashi, K.; Ito, T.; Furue, M.; Oda, Y. A novel fusion gene CRTC3-MAML2 in hidradenoma: Histopathological significance. *Hum. Pathol.* **2017**, *70*, 55–61. [[CrossRef](#)]
17. Fehr, A.; Kovács, A.; Löning, T.; Frierson, H.F.; Van Den Oord, J.J.; Stenman, G. The MYB-NFIB gene fusion—a novel genetic link between adenoid cystic carcinoma and dermal cylindroma. *J. Pathol.* **2011**, *224*, 322–327. [[CrossRef](#)]
18. Andreasen, S.; Tan, Q.; Agander, T.K.; Steiner, P.; Bjørndal, K.; Høgdaal, E.; Larsen, S.R.; Erentaite, D.; Olsen, C.H.; Ulhøi, B.P.; et al. Adenoid cystic carcinomas of the salivary gland, lacrimal gland, and breast are morphologically and genetically similar but have distinct microRNA expression profiles. *Mod. Pathol.* **2018**, *31*, 1211–1225. [[CrossRef](#)]
19. Adderley, H.; Rack, S.; Hapuarachi, B.; Feeney, L.; Morgan, D.; Hussell, T.; Wallace, A.J.; Betts, G.; Hodgson, C.; Harrington, K.; et al. The utility of TP53 and PIK3CA mutations as prognostic biomarkers in salivary adenoid cystic carcinoma. *Oral Oncol.* **2021**, *113*, 105095. [[CrossRef](#)]
20. Yusenko, M.V.; Trentmann, A.; Andersson, M.K.; Ghani, L.A.; Jakobs, A.; Arteaga Paz, M.F.; Mikesch, J.H.; Peter von Kries, J.; Stenman, G.; Klempnauer, K.H. Monensin, a novel potent MYB inhibitor, suppresses proliferation of acute myeloid leukemia and adenoid cystic carcinoma cells. *Cancer Lett.* **2020**, *479*, 61–70. [[CrossRef](#)]
21. Xie, J.; Lin, L.S.; Huang, X.Y.; Gan, R.H.; Ding, L.C.; Su, B.H.; Zhao, Y.; Lu, Y.G.; Zheng, D.L. The NOTCH1-HEY1 pathway regulates self-renewal and epithelial-mesenchymal transition of salivary adenoid cystic carcinoma cells. *Int. J. Biol. Sci.* **2020**, *16*, 598–610. [[CrossRef](#)] [[PubMed](#)]
22. Ferrarotto, R.; Mitani, Y.; McGrail, D.J.; Li, K.; Karpinets, T.V.; Bell, D.; Frank, S.J.; Song, X.; Kupferman, M.E.; Liu, B.; et al. Proteogenomic analysis of salivary adenoid cystic carcinomas defines molecular subtypes and identifies therapeutic targets. *Clin. Cancer Res.* **2021**, *27*, 852–864. [[CrossRef](#)] [[PubMed](#)]
23. Rettig, E.M.; Tan, M.; Ling, S.; Yonescu, R.; Bishop, J.A.; Fakhry, C.; Ha, P.K. MYB rearrangement and clinicopathologic characteristics in head and neck adenoid cystic carcinoma. *Laryngoscope* **2015**, *125*, E292–E299. [[CrossRef](#)] [[PubMed](#)]
24. Brayer, K.J.; Frerich, C.A.; Kang, H.; Ness, S.A. Recurrent fusions in MYB and MYBL1 define a common, transcription factor-driven oncogenic pathway in salivary gland adenoid cystic carcinoma. *Cancer Discov.* **2016**, *6*, 176–187. [[CrossRef](#)] [[PubMed](#)]
25. Mitani, Y.; Liu, B.; Rao, P.H.; Borra, V.J.; Zafereo, M.; Weber, R.S.; Kies, M.; Lozano, G.; Andrew Futreal, P.; Caulin, C.; et al. Novel MYBL1 Gene Rearrangements with Recurrent MYBL1-NFIB Fusions in Salivary Adenoid Cystic Carcinomas Lacking t(6;9) Translocations. *Clin. Cancer Res.* **2016**, *22*, 725–733. [[CrossRef](#)]
26. Kim, J.; Geyer, F.C.; Martelotto, L.G.; Ng, C.K.Y.; Lim, R.S.; Selenica, P.; Li, A.; Pareja, F.; Fusco, N.; Edelweiss, M.; et al. MYBL1 rearrangements and MYB amplification in breast adenoid cystic carcinomas lacking the MYB–NFIB fusion gene. *J. Pathol.* **2018**, *244*, 143–150. [[CrossRef](#)]
27. Yusenko, M.V.; Biyanee, A.; Andersson, M.K.; Radetzki, S.; von Kries, J.P.; Stenman, G.; Klempnauer, K.H. Proteasome inhibitors suppress MYB oncogenic activity in a p300-dependent manner. *Cancer Lett.* **2021**, *520*, 132–142. [[CrossRef](#)]
28. Lv, J.J.; Ren, M.; Cai, X.; Hu, J.; Kong, J.C.; Kong, Y.Y. Primary cutaneous adenoid cystic carcinoma: A clinicopathologic, immunohistochemical, and fluorescence in-situ hybridisation study of 13 cases. *Histopathology* **2022**, *80*, 407–419. [[CrossRef](#)]
29. Zhang, Y.; Liu, X.; Zhou, C.X.; Li, T.J. Notch activation leads to loss of myoepithelial differentiation and poor outcome in solid adenoid cystic carcinoma. *Oral Dis.* **2020**, *26*, 1677–1686. [[CrossRef](#)]
30. Fonseca, F.P.; Bingle, L.; Santos-Silva, A.R.; Lopes, M.A.; de Almeida, O.P.; de Andrade, B.A.B.; Mariano, F.V.; Kowalski, L.P.; Rangel, A.L.C.A.; Martins, M.D.; et al. Semaphorins and neuropilins expression in salivary gland tumors. *J. Oral Pathol. Med.* **2016**, *45*, 119–126. [[CrossRef](#)]
31. Khalele, B.; Laforga, J.B.; Kajo, K.; Kajová Machálek, K. Adenosquamous Carcinomas and Mucinous Adenocarcinoma of the Minor Salivary Glands: Immunohistochemical and Molecular Insights. *J. Mol. Pathol.* **2022**, *3*, 273–285. [[CrossRef](#)]

Disclaimer/Publisher’s Note: The statements, opinions and data contained in all publications are solely those of the individual author(s) and contributor(s) and not of MDPI and/or the editor(s). MDPI and/or the editor(s) disclaim responsibility for any injury to people or property resulting from any ideas, methods, instructions or products referred to in the content.